Cirrus Cloud Simulations Using WRF with Improved Radiation Parameterization and Increased Vertical Resolution

Yu Gu, K. N. Liou, S. C. Ou, and R. Fovell

Department of Atmospheric and Oceanic Sciences
Joint Institute for Regional Earth System Science and Engineering
University of California, Los Angeles
Los Angeles, CA 90095

Abstract

The capability of WRF in the simulation of cirrus clouds has been examined, with a focus on the effects of radiative processes and vertical model resolution. We incorporate in WRF a new radiation module, referred to as the Fu-Liou-Gu scheme, which is an improvement and refinement based on the Fu-Liou scheme, particularly in reference to parameterization of the single-scattering properties of ice crystal size and shape. We conducted a number of real-time WRF simulations for cirrus cases that were observed in the coastal and western United States on March 29-30, 2007, and compared with available observations from MODIS and GOES-IR images over the same areas. Simulation results show that WRF is capable of generating reasonable cirrus cloud cover and life cycle, especially those associated with frontal systems. The newly implemented Fu-Liou-Gu radiation module has been demonstrated to work well in WRF and reproduce cirrus cloud distributions observed from satellites. Using the new radiation scheme, we have illustrated improved simulations of cloud cover and ice water path for cirrus clouds. We have also demonstrated that model vertical resolution plays a significant role in cirrus cloud simulation in terms of altering vertical velocity field and the associated regional circulation.

Key word: cirrus cloud, radiation, WRF

1.Introduction

Cirrus clouds cover about 20% of the earth's surface and play an important role in the radiation field of the earth–atmosphere system and significantly affect the atmospheric thermal structure and climate [Liou 1986, 1992]. Cirrus clouds are a dynamic and thermodynamic system that involves the intricate coupling of microphysics, radiation, and dynamic processes [Gultepe and Starr 1995]. A multidimensional setting is thus required for interaction and feedback studies. A number of modeling studies have been performed to investigate cirrus cloud formation processes [e.g., Starr and Cox 1985; Heymsfield and Sabin 1989; Sassen and Dodd, 1989; Jensen et al. 1994a, b; DeMott et al. 1994]. In their pioneering work, Starr and Cox [1985] developed a two-dimensional (2D) model and showed that the effects of radiative processes and vertical transports are both significant in cirrus cloud formation and maintenance. Gu and Liou [2000] constructed a two-dimensional (2D) cirrus model to investigate the interaction and feedback of radiation, ice microphysics, and turbulence-scale turbulence, and their influence on the evolution of cirrus clouds, and reported that radiation and its interaction with microphysical and dynamical processes play an important role in the formation and evolution of these clouds.

While numerical models have been extensively used to study cirrus clouds, it is critically important to examine how reliable the models are in terms of reproducing cirrus cloud fields. For instance, one of the modeling uncertainties is the simulation of thin cirrus clouds which are important to atmospheric radiation budget [Forster et al., 2007]. Also, comparisons of the ice water content (IWC) measurements from the Earth Observing System's Microwave Limb Sounder (MLS) with those simulated from global climate models show substantial disagreements, which occur over Eastern Pacific, Atlantic ITCZs, tropical Africa, and South America [Li et al., 2005]. Improvements of model physics (e.g., radiation parameterization) and model dynamics (e.g., increasing horizontal and vertical resolution) are big issues in terms of the generation of realistic representations of cirrus cloud distribution. Among them, the parameterization of cloud/radiation processes in global and regional climate models is a complex task. Radiative transfer in the atmosphere is determined by spectrally dependent optical properties of atmospheric gases and clouds. Calculation of the radiative heating/cooling in clouds is complicated due to difficulties in parameterizing their single-scattering properties, especially those of ice clouds due to complexities in the ice crystal size, shape, and orientation which cannot be determined from the models [Liou 1986].

Model development (on model dynamics) has been confined mostly to increasing horizontal resolution; however, the vertical resolution has been usually kept at certain levels, e.g., about 20 levels for GCMs [Ruti et al, 2006]. Using a single-column model, Tompkins and Emanuel [2000] have demonstrated that the vertical distribution of water vapor in GCMs can be very sensitive to model vertical resolution. Additionally, the effects of increasing vertical resolution on climate simulation in terms of more realistic cloud spectrum and water vapor have been presented by Innes et al. [2001], Pope et al. [2001] and Spencer and Slingo [2003].

The Weather Research and Forecasting (WRF) model, a high-resolution regional model, can be used to perform real-case cirrus cloud simulations. However, its performance in terms of realistic representation of the cirrus cloud distribution in the atmosphere requires examination and in-depth investigation. The objective of this paper is to assess the WRF's capability to simulate cirrus clouds with validation from satellite observations, and to investigate the effects of improved radiation parameterization and vertical resolution on model performance and simulation.

The paper is organized as follows: Section 2 synthesizes model characteristics and new module for radiation parameterization. Section 3 describes the experiment design, real case simulations, and comparison with satellite observations. This section also presents a discussion on experiment results regarding the effects of radiation and

vertical resolution in cirrus simulations. Conclusions are given in Section 4.

2.Implementation of a New Radiation Module in WRF

The WRF model [Skamarock et al. 2007] is a fully compressible, nonhydrostatic mode (with a hydrostatic option) suitable for a broad spectrum of applications across scales ranging from a few meters to thousands of kilometers. Currently, several physics components have been included in WRF: microphysics (bulk schemes ranging from simplified physics suitable for meso-scale modeling to sophisticated mixed-phase physics suitable for cloud-resolving modeling), cumulus parameterization, longwave radiation, shortwave radiation, boundary layer turbulence, surface layer, land-surface parameterization, and subgrid scale diffusion.

For radiative transfer associated with clouds, the current schemes in WRF normally use preset tables to represent shortwave and longwave processes associated with clouds. To improve the computation of radiative transfer processes in the current WRF model, a more physically-based, consistent and efficient radiation scheme that can better resolve the spectral bands, determine the cloud optical properties, and provide more reliable and accurate radiative heating fields is needed. The new radiation module, Fu-Liou-Gu scheme [Gu et al. 2010] that we implement in WRF is a modified and improved version based on the Fu-Liou radiative transfer model. The detailed description of the model and the relevant parameters used in this scheme have been given in Fu and Liou [1992] and Fu and Liou [1993]. A combination of the delta-four-stream approximation for solar flux calculations [Liou et al. 1988] and delta-two-and-four-stream approximation for IR flux calculations [Fu et al. 1997] has been implemented in this scheme. This combination has been proven to be computationally efficient and at the same time to produce a high degree of accuracy. The incorporation of nongray gaseous absorption in multiple scattering atmospheres is based on the correlated *k*-distribution method developed by Fu and Liou [1992]. The solar and IR spectra are divided into 6 and 12 bands, respectively, according to the location of absorption bands. In the solar spectrum, absorption due to H_2O (2500-14500 cm^{-1}), O_3 (50000-14500 cm^{-1}), CO_2 (2850-5200 cm^{-1}), and O_2 (A, B, and γ bands) is taken into account. In the thermal IR region, absorption due to H_2O (0-2200 cm^{-1}), CO_2 (540-800 cm^{-1}), O_3 (980-1100 cm^{-1}), CH_4 (1100-1400 cm^{-1}), N_2O (1100-1400 cm^{-1}), and CFCs (in the 10 μm region) is included. The continuum absorption of H_2O is accounted for in the spectral region 280-1250 cm^{-1}. In addition to the principal absorbing gases listed above [Fu and Liou, 1993; Gu et al., 2003], we recently included absorption by the water vapor continuum and a number of minor absorbers in the solar spectrum, including CH_4, N_2O, NO_2, O_3, CO, SO_2, O_2-O_2, and N_2-O_2. This led to an additional absorption of solar flux in a clear atmosphere on the order of 1-3 W/m^2 depending on the solar zenith angle and the amount of water vapor employed in the calculations [Zhang et al. 2005].

The single-scattering properties for ice particles, including the extinction coefficient (β_e), the single-scattering albedo (ϖ), and the asymmetry factor (g), which are dependent on wavelength and the vertical position in the cloud, are parameterized in terms of ice water content (IWC) and mean effective size (D_e) [Liou et al. 2008]. More recently, we have also incorporated an ice microphysics parameterization to include an interactive mean effective ice crystal size (D_e) in connection with radiation parameterizations [Liou et al. 2008]. Correlation analysis between IWC and D_e has been carried out using a large set of observed ice crystal size distributions obtained from a number of cirrus field campaigns in the tropics, midlatitude, and Arctic. It is showed that IWC and D_e are well-correlated using this regional division. For the current study, parameterization of D_e for midlatitudes is employed, in which IWC ranges from ~10^{-4} – 10^{-1} g/m^3, while D_e has values from ~30-140 μm. Ice crystal shape consists of 60% bullet rosettes and aggregates, 20% hollow columns, and 20% plates for ice crystal maximum dimension (L) > 70 μum, while for L < 70 μm, the shape factor consists of 50% bullet rosettes, 25% plates, and 25% hollow columns [Baum et al., 2000; Liou et al. 2008]. Having included all the preceding ice crystal size and shape features, the Fu-Liou-Gu scheme is now an ideal tool for the simulation of radiative transfer associated with cirrus clouds in weather and climate models.

In the current Fu-Liou-Gu radiation scheme, a total of 18 aerosol types have been parameterized by employing the Optical Properties of Aerosols and Clouds (OPAC) database [d'Almeida et al., 1991; Tegen and Lacis, 1996; Hess et al., 1998], which provides the single-scattering properties for spherical aerosols computed from the Lorenz-Mie theory in which humidity effects are accounted for. The single-scattering properties of the 18 aerosol types for 60 wavelengths in the spectral region between 0.3 μm and 40 μm are interpolated into the 18 Fu-Liou spectral bands of the current radiation scheme [Gu et al., 2006; Gu et al. 2010]. Aerosol types include maritime, continental, urban, five different sizes of mineral dust, insoluble, water soluble, soot (BC), sea salt in two modes (accumulation mode and coarse mode), mineral dust in four different modes (nucleation mode, accumulation mode, coarse mode, and transported mode), and sulfate droplets. The present radiation scheme, therefore, can also be used to study direct and indirect aerosol radiative effects in addition to cirrus clouds.

3.Real Case Cirrus Cloud Simulation and Validation

3.1 Case Description

Cirrus cloud cover has been increasing over the Northeastern Pacific Ocean since 1970's, particularly during spring, due, in part, to increases in upper atmospheric humidity as well as the presence of contrails and the contrail cirrus formation and spreading as a result of trans-Pacific air traffic [Minnis et al. 2004]. Over this same region, non-frontal thin cirrus clouds were observed and reported by military pilots during test flights. For these reasons, we acquired relevant MODIS/Terra/Aqua daytime and nighttime images for March 29 and 30, 2007, over the northeastern Pacific Ocean and western United States. MODIS is a 36-channel spectro-radiometric sensor that was installed onboard both Terra and Aqua satellite platforms, which were launched in December 1999 and May 2001, respectively. Both Terra and Aqua are in sun-synchronous polar orbits with daytime equator crossings at 10:30 am and 1:30 pm LTC, respectively. Aqua is the leading platform of the A-Train constellation, which also include CALIPSO and CloudSat. MODIS has a 1 km^2 field-of-view mapping to a swath of approximately 2330 km with global data archived every day. MODIS data is divided into "granules". Each granule is composed of 2030 lines of data, and each line is composed of 1350 pixels. The MODIS cloud product contains both physical and radiative cloud properties, including cloud mask, cloud-particle phase (ice vs. water, clouds vs. snow) mask, cloud-top temperature/pressure/height, effective cloud-particle radius, and cloud optical depth. For comparison with WRF simulation results, MODIS granules over Eastern Pacific Ocean and Western United States have been examined and scenes containing widespread cirrus clouds matching the WRF domain and simulation time period have been selected.

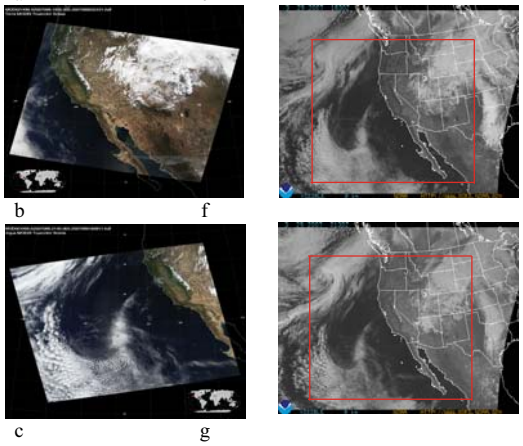

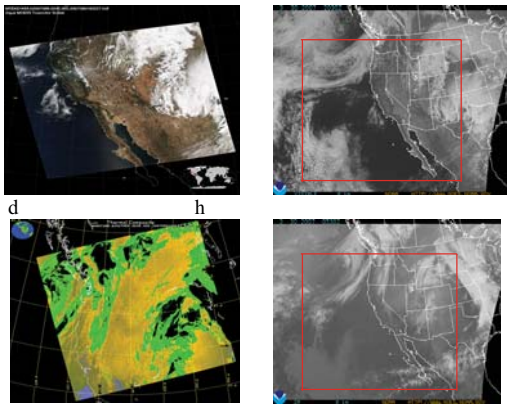

Fig. 1 Observed MODIS (a-d) and GOES-IR (e-h) images at 1800 and 2200 UTC on March 29, and 0600 and 2100 UTC on March 30, 2007.

The following is a list of MODIS images: Terra Daytime on March 29, 2007, at 1825 UTC; Aqua Daytime on March 29, 2007, at 2140 UTC, and March 30, 2007, at 2045 UTC; Terra Nighttime on March 30, 2007, at 0530 UTC, as shown in Fig. 1(a) – (d). For comparison purposes, we also acquired GOES-11 visible and IR images over the same general area from the NOAA web site for the dates and times that were close to MODIS/Terra/Aqua overpasses: March 29, 2007, at 1830 UTC; March 29, 2007, at 2130 UTC, and March 30, 2007, at 2030 UTC; Terra Nighttime on March 30, 2007, at 0530 UTC, as shown in Figs. 1(e)-(h). Both MODIS and GOES-11 observations showed the presence of frontal and non-frontal ice clouds at the dates and times listed above over coastal and western United States areas. We have selected these cases for the WRF simulations to demonstrate its capability in generating cirrus cloud patterns that can match satellite cloud images.

3.2 Experiment Design

Based on the observed cases, the model domain has been selected to center at 35 N-120 W and cover the area from 135 -105° W and 20 – 45° N. The horizontal resolution is 30 km and the bottom-top, south-north, and west-east dimensions are 28x97x112. Initial and boundary condition data used are the National Centers for Environmental Prediction (NCEP) Final (FNL) Operational Global Analysis on a 1.0x1.0 degree grid, continuously at every six hours. This product is available from the Global Forecast System (GFS) that is operational four times a day in near-real time at NCEP. We have performed 48-hour model integrations in conjunction with the observed cases.

In accordance with our research objective, i.e., to examine the ability of WRF for the simulation of cirrus clouds and to investigate the effects of radiation processes and the vertical model resolution in the simulation, we have designed the following three experiments: (1) The CTRL experiment is the control run in which the Lin ice microphysics scheme was used along with RRTM for longwave radiation and a solar radiation scheme based on a look-up table approach for cloud albedo and cloud absorption [Dudhia, 1989]. RRTM also uses preset tables [Mlawer et al., 1997] to represent longwave radiative processes primarily associated with water vapor, ozone, carbon dioxide, and cloud optical depth. A vertical resolution with 28 model levels was used in this simulation; (2) The RADI experiment is identical to CTRL, except that the Fu-Liou-Gu radiation scheme was followed; (3) In the VERT experiment, the number of model level in the RADI setup was increased from 28 to 65. Levels above 500 mb were added in order to capture the frequent occurrence of cirrus clouds at these levels.

3.3 Simulation of Cirrus Clouds and Comparison with Satellite Observations

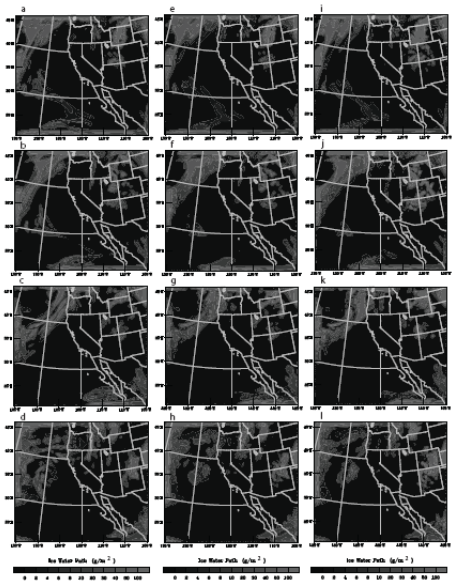

Fig. 2 Model simulated IWPs from the experiments CTRL (a-d), RADI (e-h) and VERT (i-l) at 1800 and 2200 UTC on March 29; and 0600 and 2100 UTC on March 30, 2007.

We first evaluate model performance by examining simulation results obtained from the preceding three experiments. Figures 2a-2d show the contour of simulated ice water path (IWP) from CTRL at 1800 UTC (Fig. 2a) and 2200 UTC (Fig. 2b) on March 29; and 0600 UTC (Fig. 2c) and 2100 UTC (Fig. 2d) on March 30, 2007. Figures 2e-2h and Figs. 2i-2l illustrate the simulation results determined from RADI and VERT, respectively. These results are compared with the corresponding MODIS (Fig. 1a-1d) and GOES-11 (Fig. 1e-1h) images, which display cirrus cloud cover close to the preceding times. The frame in the GOES-11 images represents the model domain. The three model simulations display the observed cirrus cloud patterns, including the clouds associated with the frontal system off the west coast and some non-frontal ice clouds to the west of southern California and Mexico. Cirrus clouds over the western United States, including Wyoming, Utah, Colorado, Arizona, and New Mexico, as shown in both MODIS and GOES-11 images, have also been well-simulated in the model. The frontal cirrus clouds off the west coast travel from west to east and move over land starting at 0600 UTC, March 30, 2007 (Fig. 1g). This migration has been well-reproduced from the model (Figs. 2c, 2g, and 2k). The cloud dissipation process when clouds move over land has been demonstrated in both satellite observations and model simulations (Fig. 1g & Figs. 2c, 2g, and 2k).

To compare with the model-simulated ice cloud water, we have obtained the total cloud water path (CWP) available from the MODIS L-2 cloud product database for the two domains: 35°-45° N and 105°-115° W, covering Wyoming, Utah, and Colorado (Region 1) and 40°-45° N and 115°-125° W, covering Oregon (Region 2) at 1800 UTC on March 29, 2007. The latter region involves semi-transparent thin cirrus clouds. MODIS datasets contain information of the optical depth and a mean effective particle size for high-level ice clouds, but not for ice water path (IWP), which is a product of IWC and cloud thickness. To obtain a reasonable IWP for comparison with model simulated values, we have followed a parameterization approach developed by Liou et al. (2008) in which the cloud optical depth, IWP, and the mean effective radius for cirrus clouds are related by the following equation:

$$t = IWP\,(e_0 + e_1 / a_e + e_2 / a_e^2),$$

where t is the cloud optical depth, IWP is the ice water path in gm/m^2, a_e is half of the mean effective ice crystal size, and e_1, e_2, e_3 are the fitting coefficients, which were determined from thousands of ice crystal size distributions collected by airborne *in situ* sampling over midlatitude and tropical areas, along with parameterization of the single-scattering properties using the data compiled by Yang et al. (2000). We determined IWPs using the above parameterization for

pixels that were identified as ice clouds based on the MODIS thermal IR cloud phase mask program. The t and a_e values have been archived for every cloudy pixel, which can be extracted from the MODIS L-2 cloud product dataset.

Table 1. Mean and standard deviation of the ice water path (IWP, g m^{-2}) for the domain of 35°-45° N and 105°-115° W (Region 1) and 40-45 N and 1150125 W (Region 2) at 1800 UTC on March 29, 2007 obtained from MODIS observations and model experiments CTRL and RADI.

Observations/Experiments	IWP (g m^{-2}) – Region 1		IWP (g m^{-2}) – Region 2	
	Mean	Std Dev	Mean	Std Dev
MODIS	38.02	106.00	23.2	48.4
CTRL	43.18	62.19	30.47	56.85
RADI	41.26	61.45	25.76	56.91

Table 1 lists IWP mean and stand deviation values for the two selected domains obtained from MODIS observations and CTRL and RADI simulation results. In terms of the IWP mean for Region 1, result from RADI, with a value of 41.26 g m^{-2} is closer to that derived from satellite observations (38.02 g m^{-2}), as compared to the value determined from CTRL (43.18 g m^{-2}). The improvement in simulated mean IWP is about 5% employing the new radiation scheme. The standard deviations from model simulations are smaller than satellite observations for IWP, indicating that model results represent a narrower IWP range. For Region 2 where semi-transparent thin cirrus clouds were present, RADI also produces a much closer agreement (25.76 g m^{-2}) with MODIS observations (23.2 g m^{-2}) for IWP, with an improvement of about 20% compared to CTRL (30.47 g m^{-2}). With the inclusion of the new radiation/cloud microphysics parameterizations in WRF, the simulated IWPs appear to be more consistent with the values derived from satellite observations, especially for thin cirrus clouds. We also compare the model simulated CWP with corresponding MODIS observations for Region 1. Figure 3 shows the histograms for CWP determined from observations and simulated from CTRL and RADI experiments for this region, where the x-axis represents the natural logarithm value of CWP. Because the model grid points are much fewer than the number of satellite observations, we compare the CWP frequency shape. The CWP distribution simulated from RADI, with a maximum frequency located between ~ 5-6 shows a closer comparison with observations than that from CTRL, which has a maximum between 7-8.

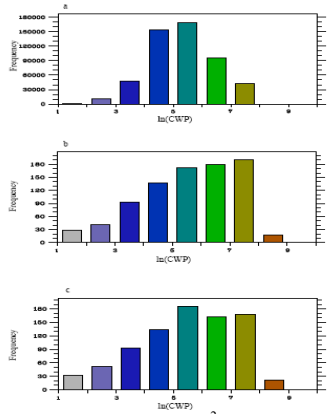

Fig. 3. Histograms of CWP (gm^{-2}) for the domain of 35°-45° N and 105°-115° W at 1800 UTC on March 29, 2007 obtained from (a) MODIS observations and model experiments (b) CTRL and (c) RADI. The x-axis represents the natural logarithm value of CWP.

Vertical resolution also plays a significant role in the simulation of cirrus clouds. With an increased vertical level, the model has been shown to produce more clouds over Wyoming, Utah, and Colorado. The mean IWP for this area (Region 1) at 1800 UTC on March 29, 2007 is about 60.53 g m^{-2}, with a standard deviation of about 152.3, larger than those obtained from CTRL and RADI. This is because an enhanced vertical resolution can significantly influence the vertical velocity field and the associated regional circulation discussed in the following. Simulated IWPs associated with the frontal system have also been enhanced with the use of a higher vertical resolution (not shown).

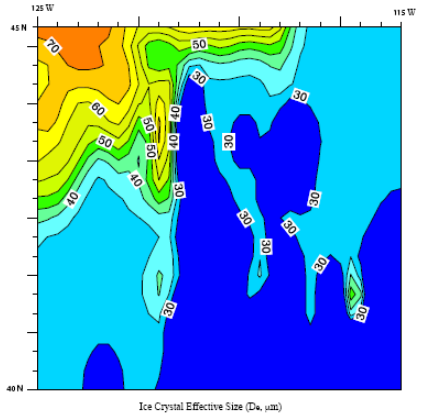

Fig. 4. Simulated column-averaged D_e from experiment RADI for the domain of 40°-45° N and 115°-125° W (Region 2) at 1800 UTC on March 29, 2007.

The present radiation and cloud microphysics parameterizations can generate a mean effective ice crystal size for direct comparison with the value inferred from satellite observations that is not available from the original radiation code in WRF. Figure 4 demonstrates this capability from a WRF simulation by showing the simulated column-averaged D_e for Region 2 at 1800 UTC on March 29, 2007. Larger Des with values between 40 – 70 μm are found in the northwest corner of this region, while smaller values occur in the southeast area in the domain. The mean D_e simulated for this semi-transparent ice cloud region is about 51.0 μm, in excellent agreement with the corresponding mean value of 51.4 μm obtained from MODIS observations. The production of an interactive ice crystal size is critical for the study of the effect of aerosols on ice cloud formation based on model simulations.

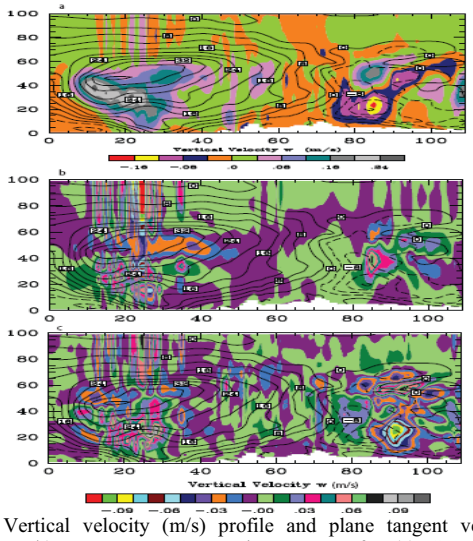

Fig. 5. Vertical velocity (m/s) profile and plane tangent velocity (contour, m/s) at 1800 UTC, March 29, 2007 for (a) CTRL, and differences in vertical velocity between the experiments (b) RADI and CTRL, and (c) VERT and RADI, at a cross-section (xz-plane) near the northern edge of the domain crossing the vortex center.

Figure 5 shows the vertical velocity together with the contour of the plane tangent velocity for CTRL (Fig. 5a) and differences in the vertical velocity between RADI and CTRL (Fig. 5b) and VERT and RADI (Fig. 5c) along the cross-section (xz-plane) near the northern edge of the domain crossing the vortex center. Corresponding to the

cyclonic circulation off the west coast, stronger ascending motions are seen in the experiments using the new radiation scheme (RADI-CTRL, Fig. 5b), which are further strengthened with the use of higher vertical resolution (VERT-RADI, Fig. 5c). These stronger vertical motions are the primary reason for the enhanced IWP in these simulations, especially in VERT. These differences are associated with changes in the radiative heating (RADI and CTRL) and the thermodynamic processes resulting from enhanced vertical model levels (VERT and RADI). The positive tangent velocities over this region indicate that the winds are coming from the south in front of the trough of the frontal system where clouds and precipitation are generated. The negative tangent velocity near the east side of the domain indicates that the winds are coming from the south and corresponds to downward velocities in the lower troposphere in this region. However, upward motion is seen above the downward velocity region, which is the primary reason for the formation of cirrus clouds in the area over Wyoming as well as a few other states to the south. Again, stronger upward air motions are found in RADI and VERT corresponding to larger IWPs in the corresponding simulations (Fig. 3). Downdraft is seen to the east of upward winds associated with regional circulation and is connected to the downward motion below the uplift. In experiments RADI and VERT, we observe that the regional uplift and downdraft have both been strengthened.

4.Conclusions

The numerical simulation of high cirrus clouds is a complex and difficult scientific task in regional weather and climate modeling studies. The capability of WRF in the simulation of cirrus clouds has been examined and validated using satellite observations, with a focus on the effects of radiative processes and vertical model resolution. We incorporate in WRF a new radiation module, referred to as the Fu-Liou-Gu scheme, which is an improvement particularly in reference to parameterization of the single-scattering properties of ice crystal size and shape. A number of real-time WRF simulations have been carried out for cirrus cases that were observed in the coastal and western United States on March 29-30, 2007, and compared with available observations from MODIS and GOES-IR images over the same areas. We have demonstrated that WRF can reproduce reasonably well the observed cirrus cloud fields and their movement and dissipation processes, especially those associated with the large scale frontal system.

Radiative processes are important in cirrus cloud simulations by affecting the vertical thermal structure and hence convection. The newly implemented radiation module, the Fu-Liou-Gu scheme, has been demonstrated to work well in the WRF model and can be used for future studies related to cirrus cloud formation and evolution and aerosol-cloud-radiation interactions, via the production of ice crystal size in addition to IWP. With the newly implemented radiation scheme, the simulations of cloud cover and IWP have been improved for cirrus clouds, with a more consistent comparison with the corresponding MODIS observations in terms of CWP and IWP means and CWP frequency distribution, especially for optically thin cirrus with an improvement of about 20% in simulated mean IWP. We have also illustrated that adding vertical layers in the original WRF above about 500 mb substantially enhances simulated cloud water due to its impact on vertical velocity field and the associated regional circulation.

***Acknowledgments*.** This research has been supported by AFOSR Grant FA9550-07-1-0408, NASA Grant NNX08AN69G, NSF Grant ATM-0924876, and JPL/NASA SURP program.

References

d'Almeida, G. A., P. Koepke, and E. P. Shettle, 1991: Atmospheric aerosols – global climatology and radiative characteristics. A. Deepak Publishing, Hampton, Virginia, 561 pp.

DeMott, Paul J., M. P. Meyers, and W. R. Cotton, 1994: Parameterization and impact of ice initiation processes relevant to numerical model simulations of cirrus clouds. *J. Atmos. Sci.,* **51,** 77–90.

Dudhia, J., 1989: Numerical study of convection observed during the winter monsoon experiment using a mesoscale two-dimensional model, *J. Atmos. Sci*., **46**, 3077-3107.

Forster, P. V., et al., 2007: Changes in atmospheric constituents and in radiative forcing, in Climate Change 2007: The Physical Science Basis. Contribution of Working Group I to the Fourth Assessment Report of the Intergovernmental Panel on Climate Change, edited by S. Solomom, D. Qin, M. Manning, Z. Chen, M. Marquis, K. B. Averyt, M. Tignor, and H. L. Miller, pp. 129-234, Cambridge University Press, Cambridge, United Kingdom and New York, NY, USA.

Fu, Q., and K. N. Liou, 1992: On the correlated k-distribution method for radiative transfer in nonhomogeneous atmospheres, *J. Atmos. Sci*., **49**, 2139–2156.

__, and K. N. Liou, 1993: Parameterization of the radiative properties of cirrus clouds, *J. Atmos. Sci.*, **50**, 2008–2025.

Fu, Q., K. N. Liou, M. C. Cribb, T. P. Charlock, and A. Grossman, 1997: Multiple scattering parameterization in thermal infrared radiative transfer, *J. Atmos. Sci*., **54**, 2799-2812.

Gu, Y. and K. N. Liou, 2000: Interaction of radiation, microphysics, and turbulence in the evolution of cirrus clouds, *J. Atmos. Sci*., **57**, 2463-2479.

Gu, Y., J. Farrara, K. N. Liou, and C. R. Mechoso, 2003: Parameterization of cloud-radiation processes in the UCLA general circulation model. *J. Climate*, **16**, 3357–3370.

Gu, Y., K. N. Liou, Y. Xue, C. R. Mechoso, W. Li, and Y. Luo, 2006: Climatic effects of different aerosol types in China simulated by the UCLA general circulation model. *J. Geophys. Res.,* **111**, D15201, doi:10.1029/2005JD006312.

Gu, Y., K. N. Liou, W. Chen, H. Liao, 2010: Direct climate effect of black carbon in China and its impact on dust storms, *J. Geophys. Res.* (in press).

Gultepe, I., and D. O'C. Starr, 1995: Dynamical structure and turbulence in cirrus clouds: Aircraft observations during FIRE. *J. Atmos. Sci.,* **52,** 4159–4182.

Heymsfield, A. J., and R. M. Sabin, 1989: Cirrus crystal nucleation by homogeneous freezing of solution droplets. *J. Atmos. Sci.,* **46,** 2252–2264.

Hess, M., P. Koepke, and I. Schult, 1998: Optical properties of aerosols and clouds: The software package OPAC. *Bull. Am. Met. Soc.,* **79**, 831-844.

Inness, P. M., J. M. Slingo, S. J. Woolnough, R. B. Neale, and V. D. Pop, 2001: Organization of tropical convection in a GCM with varying vertical resolution: Implications for the simulation of the Madden-Julian oscillation, *Clim. Dyn*., **17**, 777-793.

Jensen, E. J., O. B. Toon, D. L. Westphal, S. Kinne, and A. J. Heymsfield, 1994a: Microphysical modeling of cirrus: 1. Comparison with 1986 FIRE IFO measurements. *J. Geophys. Res.,* **99,** 10 421–10 442.

——**,** 1994b: Microphysical modeling of cirrus: 2. Sensitivity studies. *J. Geophys. Res.,* **99,** 10 443– 10 454.

Li, J.-L., D. E. Waliser, J. H. Jiang., D. L. Wu, W. Read, J. W. Waters, A. M. Tompkins, L. J. Donner, J.-D. Chern, W.-K. Tao, R. Atlas, Y. Gu, K. N. Liou, A. Del Genio, M. Khairoutdinov, and A. Gettelman, 2005: Comparisons of EOS MLS cloud ice measurements with ECMWF analyses and GCM simulations: Initial results, *Geophys. Res. Lett*., **32**, L18710, doi:10.1029/2005GL023788.

Liou, K. N., 1986: Influence of cirrus clouds on weather and climate processes: A global perspective, *Mon. Wea. Rev*., **114**, 1167-1198.

——, 1992: Radiation and Cloud Processes in the Atmosphere, Oxford University Press, 487 pp.

—, Q. Fu., and T. P. Ackerman, 1988: A simple formulation of the delta-four-stream approximation for radiative transfer parameterizations. *J. Atmos. Sci*., **45**, 1940-1947.

—, Y. Gu, Y. Que, and G. MacFarquhar, 2008: On the correlation between ice water content and ice crystal size and its application to radiative transfer and general circulation models. *Geophys. Res. Lett.*, **35**, L13805, doi:10.1029/2008GL033918.

Minnis, P., J. K. Ayers, R. Palikonda, and D. Phan, 2004: Contrails, cirrus trends, and climate, *J. Climate*, **17**, 1671-1685.

Mlawer, E. J., S. J. Taubman, P. D. Brown, M. J. Iacono, and S. A. Clough, 1997: Radiative trans-fer for inhomogeneous

atmosphere: RRTM, a validated correlated-k model for the long-wave, *J. Geophys. Res*., **102** (D14), 16663-16682.

Pope, V. D., J. A. Pamment, D. R. Jackson, and A. Slingo, 2001: The representation of water vapor and its dependence on vertical resolution in the Hadley Centre Climate Model, *J. Clim*., **14**, 3065-3085.

Ruti, P. M., D. Di Rocco, and S. Gualdi, 2006: Impact of increased vertical resolution on simulation of tropical climate, *Theor. Appl. Clim*., **85**, 61-80.

Sassen, K., and G. C. Dodd, 1989: Haze particles nucleation simulations in cirrus clouds, and applications for numerical modeling and lidar studies. *J. Atmos. Sci.,* **46,** 3005–3014.

Spencer, H., and J. M. Slingo, 2003: The simulation of peak and delayed ENSO teleconnections. *J. Clim*., **16**, 1757-1774.

Starr, D. O'C., and S. K. Cox, 1985: Cirrus clouds. Part I: A cirrus cloud model. *J. Atmos. Sci.,* **42,** 2663–2681.

Tegen, I., and A. A. Lacis, 1996: Modeling of particle size distribution and its influence on the radiative properties of mineral dust aerosol. *J. Geophys. Res.*, **101**, 19237-19244.

Tompkins, A. M., and K. A. Emanuel, 2000: The vertical resolution sensitivity of simulated equilibrium tropical temperature and water vapor profiles. *Quart. J. Roy. Meteor. Soc*., **126**, 1219-1238.

Yang, P., K. N. Liou, K. Wyser, and D. Mtichell, 2000: Parameterization of the scattering and absorption properties of individual ice crystals. *J. Geophys. Res.*, **105**, 4699–4718.

Zhang, F., Q. Zeng, Y. Gu, and K. N. Liou, 2005: Parameterization of the absorption of H_2O continuum, CO_2, O_2, and other trace gases in the Fu-Liou solar radiation program. *Advances in Atmos. Sci.,* **22**, 545-558.